19th Brazilian Congress of Thermal Sciences and Engineering
November 6th–10th, 2022, Bento Gonçalves - RS - Brazil

ENC-2022-0402
Axisymmetric Two-phase Finite Element Simulation Using a Front Tracking Method on an Unstructured Mesh

Daniel B. V. Santos
Gustavo R. Anjos
Federal University of Rio de Janeiro, Rio de Janeiro, Brazil
daniel.barbedo@coppe.ufrj.br, gustavo.rabello@coppe.ufrj.br

Abstract. *The goal of this research is to accurately depict two-phase dynamics, using axisymmetric finite element numerical simulation. To achieve this goal, the incompressible Navier-Stokes equations for two-phase flows, are solved through the Finite Element Method (FEM), using a two-phase separation strategy where there are two distinct meshes, one for the two-phase fluid and one for the interface. The mini element is utilized in order to respect the LBB condition, and avoid artificial stabilization terms in the fluid motion equations. The non-linear convective term on the Navier-Stokes equation is solved by applying a first order semi-Lagrangian scheme. Of the two meshes used, the fluid mesh has several finite element nodes and is fixed, not requiring any re-meshing or interference during the simulation. The interface mesh moves and requires re-meshing, but has quite fewer points relative to the fluid mesh, and so the movement and re-meshing computational costs are negligible. The fluid and interface meshes are decoupled; the only link between them is the interface mesh position update, based on the velocity fields obtained from the fluid mesh, through the finite element solution. Fluid properties are smoothed over a defined thickness of the fluid interfaces, thus avoiding numerical instability. Surface tension is implemented using the well-known continuum surface tension model, using the Laplace-Beltrami operator for curvature computation. As validation for the discussed approach, three test cases will be presented. The static droplet, where a droplet stays still while surface tension is balanced by pressure; the oscillating droplet, where a droplet starts in elliptical shape, and oscillates; and the gravity driven bubbles, where bubbles rises inside a quiescent fluid, dominated by gravity force, all presenting satisfactory results according to the available literature.*

Keywords: *Two-phase Flow, Gravity Driven Bubble, Oscillating Bubble, Laplace-Beltrami, Decoupled Fluid Interface.*

1. INTRODUCTION

Two-phase flow is present in a broad range of industrial applications, such as cooling of electronic components like microprocessors and data banks, the extraction and refinement of oil and gas Jia Liu (2020), power electronics in hybrid cars, nuclear reactor components, medical X-ray equipment and more Chirag R. Kharangate (2017). It is also very physics rich phenomena, which can involve heat transfer, evaporation, condensation, capillarity effects, movement of bubbles, all in a single problem. As such, it is a complex phenomenon to model, be it experimentally or numerically.

Two-phase flow has several branches of research, with none elected the principal method of solving the problem. As such, there's many differing approaches to the problem, such as D.L. Sun (2010) who extended the VOSET method, which is a combination of the Level Set and Volume of Fluid, to three dimensions, using the Piecewise Linear Interface Construction (PLIC) to reconstruct the interface shape. Kong Ling (2015) expands on D.L. Sun (2010)'s work, extending PLIC to 3D cases and using a geometric approach to compute the level-set function, with the intent of simplifying the extension of VOSET from 2D to 3D. Andrea Ferrari (2017) proposed a method that combines both the Level Set (LS) and Volume of Fluid (VOF), called Flexible Coupled Level Set and Volume of Fluid (flexCLV), designed to benefit from the good interface topology offered by the Level Set method. Mathieu Labois (2017) presented a multi-phase formulation with a pressure-based approach, using the 4+-equation model, for compressible flows. Tong Qin (2013) investigated the interaction between a deformable bubble and a rigid wall, through direct numerical simulation, using the ALE method to simulate the bubble interface.

E. Gros (2018) simulates a two-phase fluid flow with heat and mass transfer, using the finite element method combined with the ALE framework. Baolin Tian (2020) developed an ALE method for the five-equation model. The ALE model used is two-stage, with a Lagrangian phase and a rezone-remap phase. Zekang Cheng (2020) solved the incompressible Navier-Stokes equations for a two dimensional domain by discretizing them by Taylor-Hood elements, using an ALE finite

element method, where the mesh conforms to the fluid interface, and re-meshes when the interface suffers deformations, following its evolution. Anjos *et al.* (2020) presented an ALE finite element method for simulation of axisymmetric two-phase flows, with dynamic boundaries and interface tracking. In his work, the mesh points move to give a detailed description of the fluid interfaces while using adaptive mesh refining and re-meshing to guarantee high quality mesh elements.

In this work, we present a front-tracking method using the finite element method on unstructured meshes, which allow diverse geometric shapes to be simulated. A two-phase flow is simulated using the "one-fluid" approach, and the interface between the fluids is a separate, one dimensional mesh, not coupled to the fluid mesh, delimiting the bubble, droplet or limit between fluids. Surface tension force is computed through the curvature, which is calculated using the Laplace-Beltrami operator, and then transformed into a volume force through the continuum surface force model, as proposed by J. U. Brackbill and Zemach (1991). Three examples are presented for validation. The static droplet is a case where a droplet of fluid stays still in quiescent fluid. In this case one can measure the pressure change from inside to outside the droplet, and evaluate the parasitic currents intensity. In the oscillating droplet example, a droplet initially shaped like an ellipse, is released inside a fluid without gravity. The surface tension force makes it oscillate around its equilibrium radius. The frequency and amplitude of the oscillations can be compared to analytical results. Finally, in the gravity driven bubbles example one can compare the simulated bubble shape to a bubble generated in an experiment, under the same simulated conditions.

2. METHODOLOGY

To describe the flow fields, one needs to solve the Navier-Stokes equations. The chosen approach is the "one-fluid", where both fluid phases are described by a single set of equations, where the properties change spatially. The $\mathbf{f_{st}}$ term is added to the momentum equation to represent the surface tension forces, as a volumetric force. The Navier-Stokes equations in their non-dimensional form for an incompressible flow are given as:

$$\nabla \cdot \mathbf{v} = 0 \tag{1}$$

$$\rho(\mathbf{x})\left(\frac{\partial \mathbf{v}}{\partial t} + \mathbf{v}\cdot\nabla\mathbf{v}\right) = -\nabla p + \frac{1}{Re}\nabla\cdot\mu(\mathbf{x})\left(\nabla\mathbf{v} + \nabla\mathbf{v}^T\right) + \frac{1}{We}\mathbf{f_{st}} + \rho(\mathbf{x})\mathbf{g} \tag{2}$$

$\rho(x)$ is the fluid's density, $\mathbf{v}$ is the fluid's velocity vector, p is the pressure, Re is the flow's Reynolds number, $\mu(x)$ is the fluid's viscosity, We is the Weber number and g is the gravity acceleration. The fluid properties are considered constant over time, but change with position vector x.

The convective term in the momentum equation is often a source of instability, and it was modeled explicitly by a first order semi-Lagrangian scheme, as described by André Robert (1984).

The term describing the surface tension forces, $\mathbf{f_{st}}$, is modeled as a volumetric force, as proposed by J. U. Brackbill and Zemach (1991), using the continuum surface model. It is given by

$$\mathbf{f_{st}} = \kappa\nabla H \tag{3}$$

and is a function of the interface curvature, κ. The curvature can be calculated by using the Laplace-Beltrami operator, as reported by Hysing (2005). The other term in Eq. (3), ∇H, is the Heaviside function. The Heaviside function works as a color function for the continuum surface model, which models the surface tension as a volumetric force. It's also used to define smooth properties over a fictional interface thickness. The abrupt change in properties, μ and ρ, across the phase's interface make the finite element simulation unstable, and one solution to this issue is to create a fictional interface thickness, where the properties are smoothed over as the position vector moves from phase to the other.

The properties are calculated as follows, over the entire fluid domain,

$$\rho(\mathbf{x}) = \rho_1 H(\mathbf{x}) + \rho_2(1 - H(\mathbf{x})) \qquad \mu(\mathbf{x}) = \mu_1 H(\mathbf{x}) + \rho_2(1 - H(\mathbf{x})) \tag{4}$$

The Heaviside itself is given by

$$H = \begin{cases} 1, & \text{if } d > \epsilon \\ 0, & \text{if } d < -\epsilon \\ 1 - 0.5\left[1 + \dfrac{d}{\epsilon} + \dfrac{1}{\pi}sin\big(\pi d/\epsilon\big)\right], & \text{otherwise} \end{cases} \tag{5}$$

where ϵ is the interface thickness, d is the smallest distance from the interface to a given point evaluated by x.

Fluid Mesh Nodes/Interface Nodes	$Max(V_x)$	$Max(V_y)$
17596 / 43	2.31×10^{-13}	1.62×10^{-13}
17596 / 159	4.20×10^{-13}	1.49×10^{-13}
17596 / 643	4.10×10^{-8}	1.02×10^{-8}
49049 / 43	1.88×10^{-12}	1.49×10^{-12}
49049 / 159	2.44×10^{-12}	1.82×10^{-12}
49049 / 643	8.75×10^{-9}	1.81×10^{-8}

Table 1. Static droplet spurious velocities order of magnitude for all mesh configurations. The first column quantifies the nodes on fluid mesh and the interface mesh. The second and third columns show the maximum absolute value for horizontal and vertical velocities, respectively. The optimal values are zero.

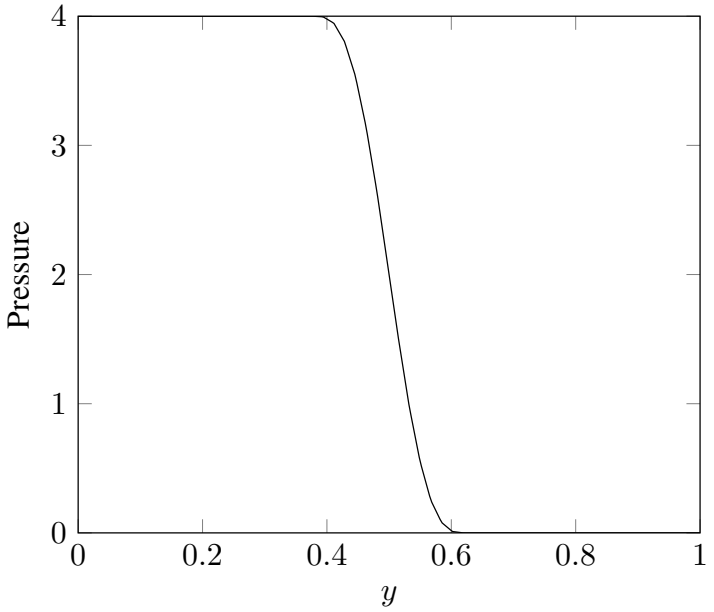

Figure 1. Static Droplet. Pressure graph, from droplet center to edge of fluid domain.

3. NUMERICAL MODEL

The Navier-Stokes equations are solved using the finite element method. The chosen finite element is the "mini" element, a triangular four node element, with one node in each triangle vertex and one node in the triangle's center of mass. The velocity field is calculated on all four nodes, but the pressure is evaluated only on the triangle vertices. The mini element is used for both fluid phases, in fact, no distinction is made between phases, except for the fluid properties at a point. The fluid interface is represented by a linear mesh, and this mesh is used for curvature calculations, which in turn are used to evaluate the surface tension forces, and as reference for the Heaviside functions parameters.

The meshes are decoupled from each other, the fluid mesh is fixed, and the interface mesh's position is updated in each iteration, using the velocity fields obtained from the finite element solution and the time increment. The new values for the interface mesh position and curvature are in turn used to update the fluid properties and surface tension force values.

The fluid properties are constant inside an element, but their values can vary between the values of the first fluid and the values of the second fluid, if the element is inside the fictional interface thickness.

4. NUMERICAL RESULTS

In this section, the examples chosen to validate the proposed methodology are show. The static droplet, the oscillating droplet and the rising bubble are presented, and compared to existing data. The static droplet consists in simulating an static droplet, with no external fluid velocity or influence from gravity. In this example, no movement or velocity is expected from the droplet. The oscillating droplet example consists of an ellipsis oscillating around its spherical shape with no influence from gravity forces. The droplet's amplitude and damping can be discovered analytically and used as validation. Finally, the rising bubble example consists of an lighter fluid bubble inside a heavier fluid, subject to gravity forces. The bubble's shape can be evaluated qualitatively and compared to experimental data.

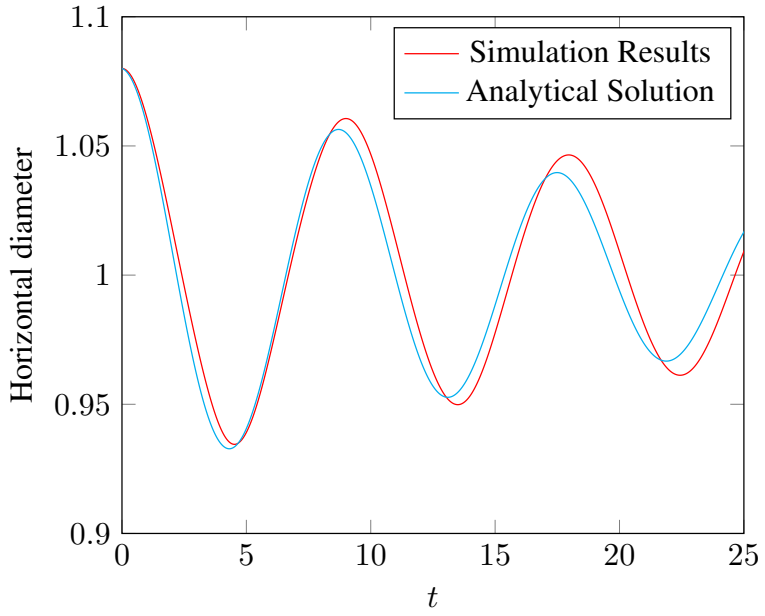

Figure 2. Oscillating Droplet Diameter. The variation in the droplet's diameter in red can be seen in this figure, plotted against the analytical solution in cyan. $Re = 500$ and $We = 125$

4.1 Static Droplet

For this example, a domain of non dimensional height = 1 and length = 2 was set up, to simulate a droplet of non dimensional radius $r = 0.5$. The simulation was run with $We = 1$, $Re = 1$, $\Delta t = 0.01$ for over 300 iterations. The droplet's properties are $\mu = 1$ and $\rho = 1$, and the outside fluid's properties $\mu = 0.01$ and $\rho = 0.001$.

In this case, since there's no velocity, the only non zero terms of the momentum equation are the pressure and surface tension forces. Thus we expect a drop in pressure from one phase to the other that can be obtained directly from Laplace's equation

$$\Delta p = \frac{\kappa}{We} \tag{6}$$

For a droplet of radius $R = 0.5$, the pressure drop should be equal to $\Delta p = 4$, and the simulation results can be observed in figure 1. All simulations executed had results similar enough that they produced the same graph at current resolution. The graph shows the pressure values from the droplet's center to the edge of the fluid mesh for.

As an effort to examine the spurious velocities, two fluid meshes were executed, with 17596 and 49049 nodes, with three different interface meshes with 43, 159 and 643 nodes. In table 1 one can compare the maximum order of magnitude for the spurious velocities value across all iterations. This value should be as close to zero as possible, since no velocity is expected for this example.

4.2 Oscillating Droplet

This example is comprised of an ellipsoid droplet, released in quiescent fluid with no gravity forces acting upon it. The surface tension force induces movement on the droplet, making it oscillate around its spherical equilibrium radius, the radius of a sphere of same volume as the initial ellipse, while being damped by the fluid's viscosity. Its shape and horizontal velocity field can be observed in figure 3. The oscillations amplitude and frequency can be computed analytically, and can be seen in figure 2 for the chosen Reynolds number and fluid properties.

The droplet was placed inside a domain with height = 1 and length = 2, the droplet's major radius was chosen to be 0.54 and its minor radius 0.481, as to preserve the equilibrium radius of R = 0.5. The properties chosen were $We = 125$ and $Re = 500$. The droplet's density and viscosity were set to $\rho = 1$ and $\mu = 1$, and the outer fluid's properties are $\rho = 0.001$ and $\mu = 0.001$. The simulation ran for 2500 iterations with $\Delta t = 0.01$

4.3 Rising Bubbles

A domain of non dimensional length = 4 and height = 1 was set up. The Weber number set to $We = 10$ and Reynolds number set to $Re = 35$. The inside fluid properties are $\mu = 0.1$ and $\rho = 0.1$. The outer fluid's properties are $\mu = 1$ and $\rho = 1$. Gravity forces are directed to the left for convenience. The simulation had 24462 nodes for the fluid mesh and

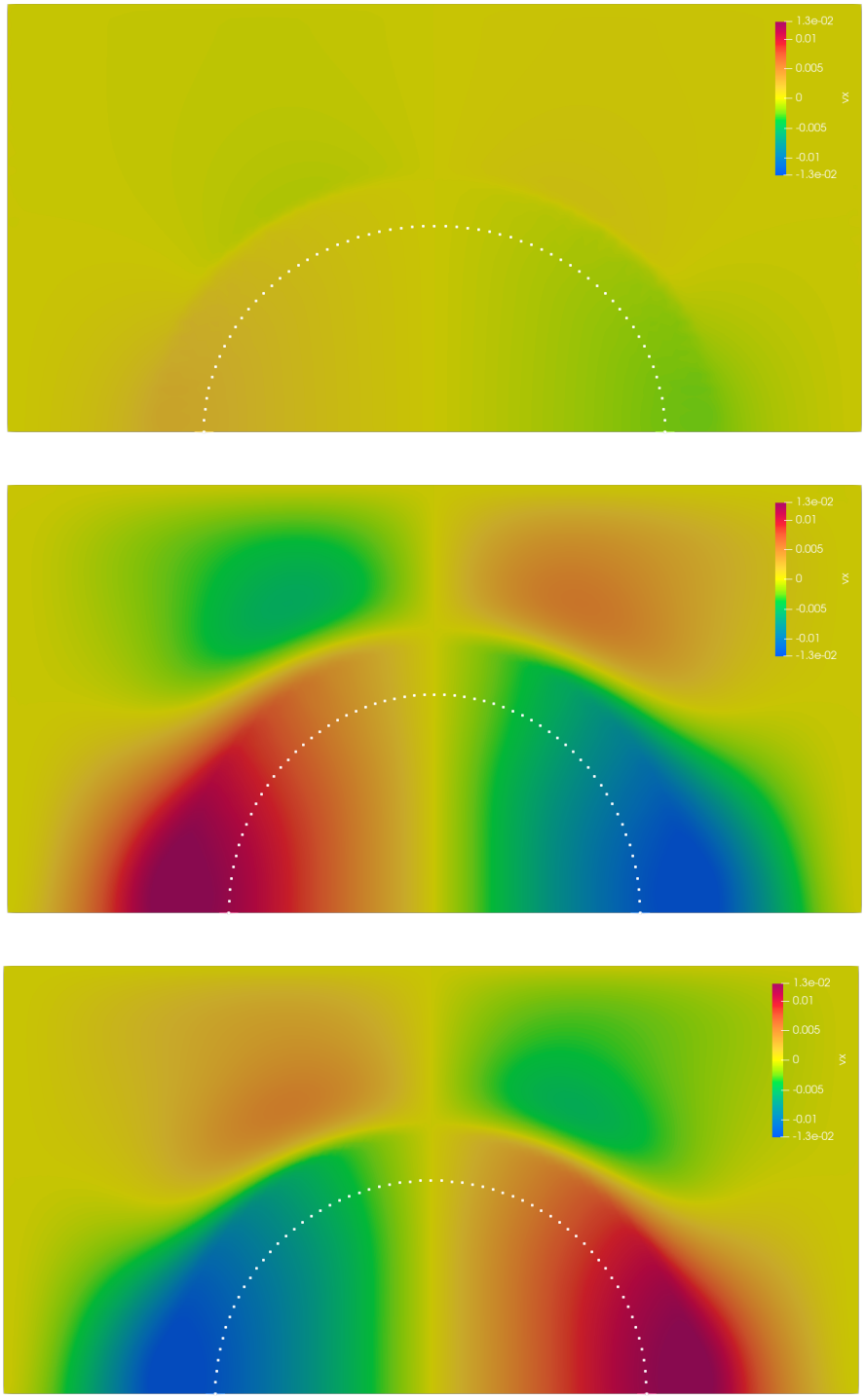

Figure 3. Oscillating Droplet. Droplet shape and horizontal velocity field at iteration 0, 1249, and 2499, equivalent to t = 0, t = 12,5 and t = 25. Red indicates a positive horizontal velocity, while blue indicates a negative horizontal velocity. The color inversion indicates the bubble's oscillation. $\Delta t = 0.01$. $We = 125$ and $Re = 500$. 17596 nodes, with $\rho_{in}/\rho_{out} = 1000$ and $\mu_{in}/\mu_{out} = 1000$

159 interface nodes. The expected bubble geometry considering the chosen simulation parameters is an ellipsoidal bubble cap, and this is what can be observed in figure 4.

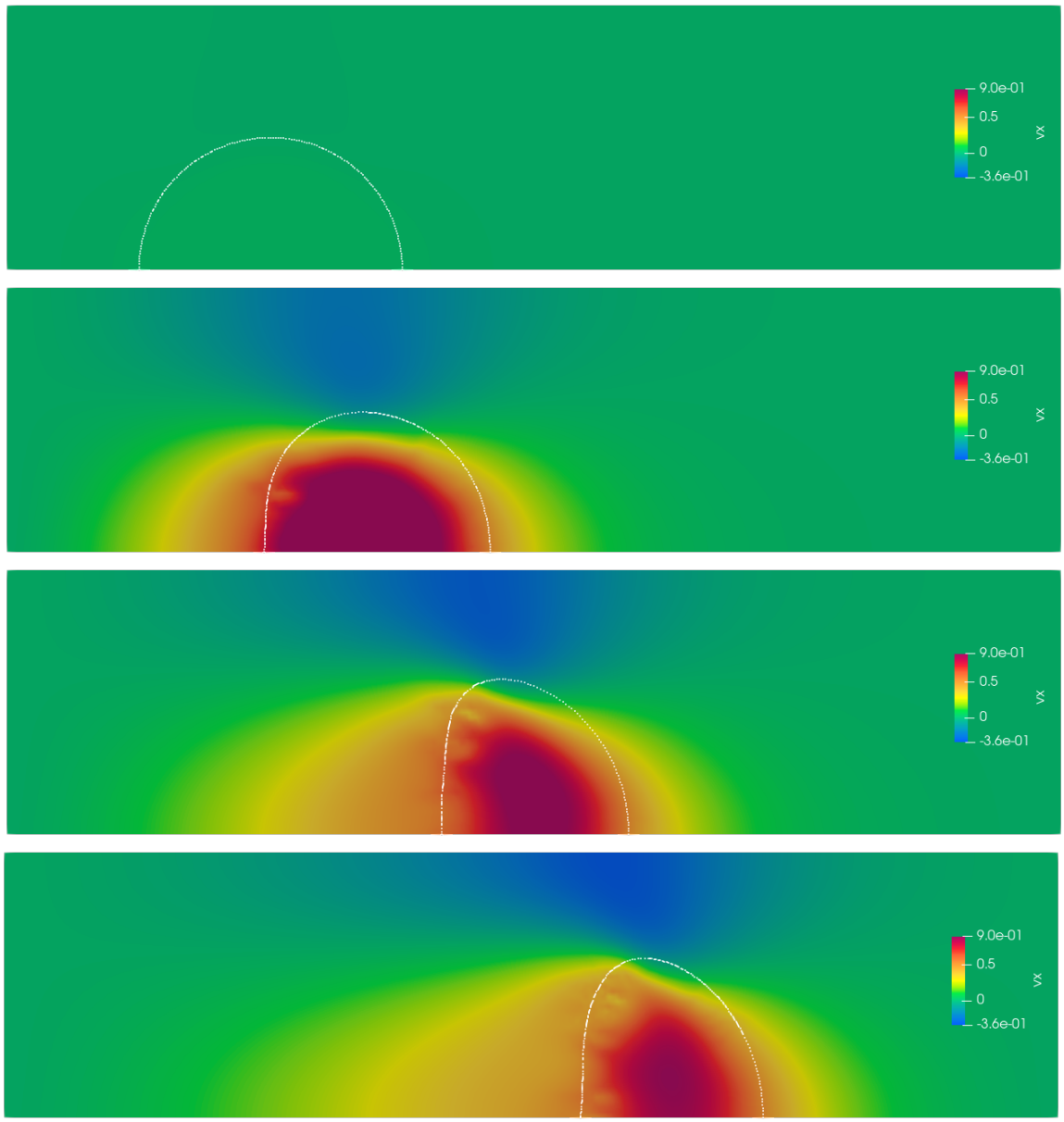

Figure 4. Rising Bubble. Droplet shape and horizontal velocity field at iteration 0, 199, 399 and 599, equivalent to t = 0, t = 1, t = 2, and t = 3. $\Delta t = 0.005$. $We = 10$ and $Re = 35$. 29462 nodes, with $\rho_{in}/\rho_{out} = 0.1$ and $\mu_{in}/\mu_{out} = 0.1$. The color red indicates a positive horizontal velocity, blue indicates negative horizontal velocity, while green indicates a value of zero

Additionally, a Taylor bubble was simulated, with $Re = 100$, $We = 50$, the inside fluid properties being $\mu = 0.01$ and $\rho = 0.001$. The outer fluid's properties are $\mu = 1$ and $\rho = 1$. In figure 5, one can observe the initial bubble shape chosen, a rectangular bubble, with height = 0.32 and length = 1. The fluid domain's dimensions are height = 0.5 and length = 4. As the surface tension forces and gravity act upon it, the bubble starts taking the familiar Taylor bubble shape. The simulation was executed with 14480 nodes for the fluid mesh, and 83 elements for the interface mesh, over 800 iterations.

5. CONCLUSION

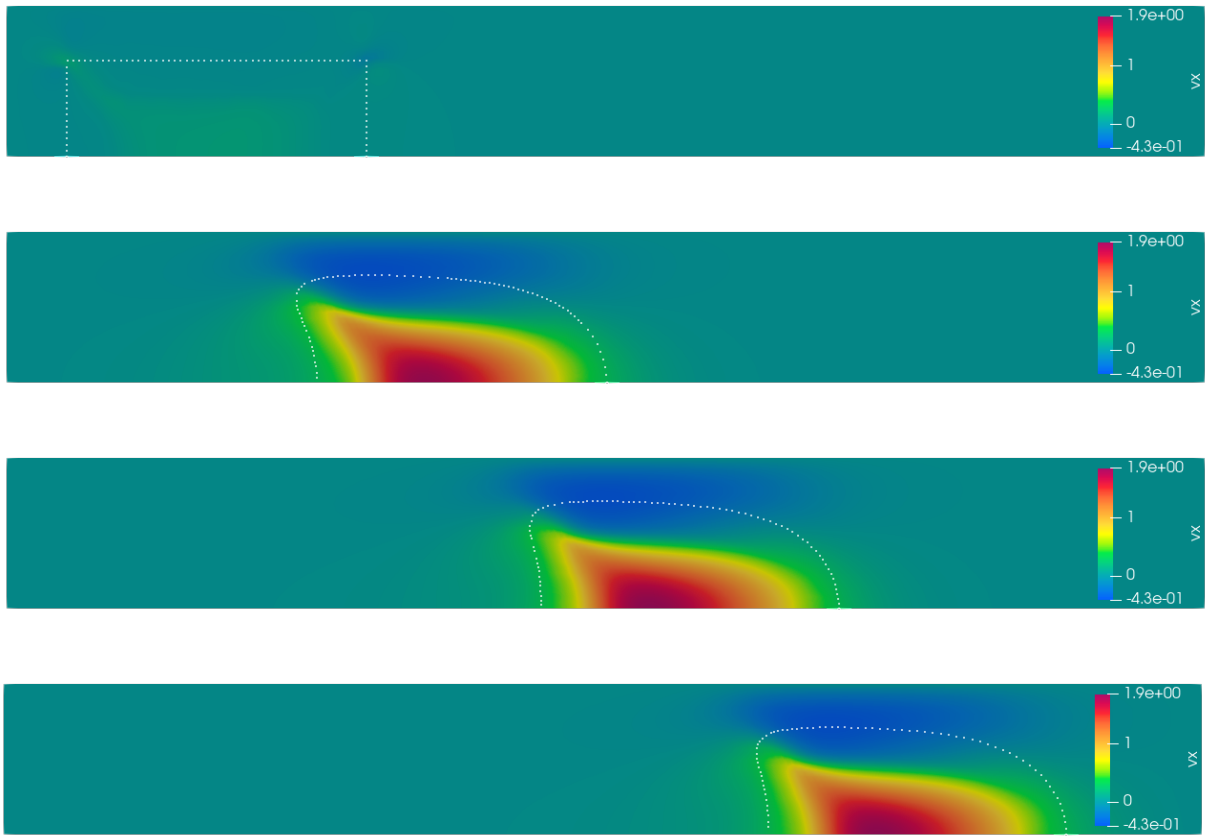

Figure 5. Taylor Bubble. Droplet shape and horizontal velocity field at iteration 0, 266, 533 and 799, equivalent to t = 0, t = 1.33, t = 2.66, and t = 4. The initial droplet shape is a rectangle of height = 0.32 and length = 1. $\Delta t = 0.005$. $We = 50$ and $Re = 100$. 14480 nodes, with $\rho_{in}/\rho_{out} = 0.001$ and $\mu_{in}/\mu_{out} = 0.01$. The color red indicates a positive horizontal velocity, blue indicates negative horizontal velocity, while green indicates a value of zero

The proposed methodology to simulate two-phase flow, a front tracking strategy with a decoupled interface mesh, with the Laplace-Beltrami operator for curvature calculation and continuum surface force method showed itself solid. The results obtained on the static droplet example show that contrary to expectation, too much refining on the interface mesh can be detrimental to simulation accuracy, and that a relatively small number of interface nodes is enough to guarantee stability and accuracy. The oscillating droplet example matched analytical results to reasonable precision, and one can expect accuracy to improve with further fluid mesh refinement. The rising bubbles presented satisfactory qualitative results, adopting the ellipsoidal cap shape and the Taylor bubble's "bullet" shape, which were expected. The use of asymmetric coordinates allows for simulation of real world scenarios, and it will be continually used in this research as validation for the upcoming tridimensional implementation of the methodology.

6. REFERENCES

Andrea Ferrari, Mirco Magnini, J.R.T., 2017. "A flexible coupled level set and volume of fluid (flexclv) method to simulate microscale two-phase flow in non-uniform and unstructured meshes". *International Journal of Multiphase Flow*, Vol. 91, pp. 276–295. doi:http://dx.doi.org/10.1016/j.ijmultiphaseflow.2017.01.017.

André Robert, Tai Loy Lee, H.R., 1984. "A semi-lagrangian and semi-implicit numerical integration scheme for multilevel atmospheric models". *Monthly Weather Review*, Vol. 113, p. 388.

Anjos, G., Mangiavacchi, N. and Thome, J., 2020. "An ale-fem method for two-phase flows with dynamic boundaries". *Computer Methods in Applied Mechanics and Engineering*, Vol. 362, p. 112820. ISSN 0045-7825. doi:https://doi.org/10.1016/j.cma.2020.112820. URL `http://www.sciencedirect.com/science/article/pii/S0045782520300013`.

Baolin Tian, L.L., 2020. "A five-equation model based global ale method for compressible multifluid and multiphase flows". *Computers and Fluids*, Vol. 214, p. 104756. doi:https://doi.org/10.1016/j.compfluid.2020.104756.

Chirag R. Kharangate, I.M., 2017. "Review of computational studies on boiling and condensation". *International Journal of Heat and Mass Transfer*, Vol. 108, pp. 1164–1196. doi:http://dx.doi.org/10.1016/j.ijheatmasstransfer.2016.12.065.

D.L. Sun, W.T., 2010. "A coupled volume-of-fluid and level set (voset) method for computing incompressible two-phase flows". *International Journal of Heat and Mass Transfer*, Vol. 53, pp. 645–655. doi: http://dx.doi.org/10.1016/j.ijheatmasstransfer.2009.10.030.

E. Gros, G. Anjos, J.T., 2018. "Moving mesh method for direct numerical simulation of two-phase flow with phase change". *Applied Mathematics and Computation*, Vol. 339, pp. 636–650. doi: https://doi.org/10.1016/j.amc.2018.07.052.

Hysing, S., 2005. "A new implicit surface tension implementation for interfacial flows". *International Journal for Numerical Methods in Fluids*, Vol. 51, pp. 659–672. doi:10.1002/fld.1147.

J. U. Brackbill, D.B.K. and Zemach, C., 1991. "A continuum method for modeling surface tension". *Journal of Computational Physics*, Vol. 100, pp. 335–354. doi:https://doi.org/10.1016/0021-9991(92)90240-Y.

Jia Liu, X.L., 2020. "Numerical evaluation on multiphase flow and heat transfer during thermal stimulation enhanced shale gas recovery". *Applied Thermal Engineering*, Vol. 178, p. 155554. doi: https://doi.org/10.1016/j.applthermaleng.2020.115554.

Kong Ling, Z.H.L., 2015. "A three-dimensional volume of fluid & level set (voset) method for incompressible two-phase flow". *Computers & Fluids*, Vol. 118, pp. 293–304. doi:http://dx.doi.org/10.1016/j.compfluid.2015.06.018.

Mathieu Labois, C.N., 2017. "Non-conservative pressure-based compressible formulation for multiphase flows with heat and mass transfer". *International Journal of Multiphase Flow*, Vol. 96, pp. 24–33. doi: http://dx.doi.org/10.1016/j.ijmultiphaseflow.2017.07.004.

Tong Qin, Saad Ragab, P.Y., 2013. "Axisymmetric simulation of the interaction of a rising bubble with a rigid surface in viscous flow". *International Journal of Multiphase Flow*, Vol. 52, pp. 60–70. doi: http://dx.doi.org/10.1016/j.ijmultiphaseflow.2013.01.001.

Zekang Cheng, Jie Li, C.Y.L., 2020. "An exactly force-balanced boundary-conforming arbitrary-lagrangian-eulerian method for interfacial dynamics". *Journal of Computational Physics*, Vol. 408, p. 109237. doi: https://doi.org/10.1016/j.jcp.2020.109237.

7. RESPONSIBILITY NOTICE

The authors are solely responsible for the printed material included in this paper.